

DETC2010/28061

**DRAFT: GEOMETRIC, SPATIAL PATH TRACKING USING NON-REDUNDANT  
MANIPULATORS VIA SPEED-RATIO CONTROL**

**Satyajit Ambike**

Department of Mechanical Engineering  
The Ohio State University  
Columbus, Ohio, 43210  
Email: ambike.1@buckeyemail.osu.edu

**First Coauthor\***

**James P. Schmiedeler and Michael M. Stanisic**  
Aerospace and Mechanical Engineering  
University of Notre Dame  
Notre Dame, Indiana, 46556  
schmiedeler.4, stanisic.1@nd.edu

**ABSTRACT**

*Path tracking can be accomplished by separating the control of the desired trajectory geometry and the control of the path variable. Existing methods accomplish tracking of up to third-order geometric properties of planar paths and up to second-order properties of spatial paths using non-redundant manipulators, but only in special cases. This paper presents a novel methodology that enables the geometric tracking of a desired planar or spatial path to any order with any non-redundant regional manipulator. The governing first-order coordination equation for a spatial path-tracking problem is developed, the repeated differentiation of which generates the coordination equation of the desired order. In contrast to previous work, the equations are developed in a fixed global frame rather than a configuration-dependent canonical frame, providing a significant practical advantage. The equations are shown to be linear, and therefore, computationally efficient. As an example, the results are applied to a spatial 3-revolute mechanism which tracks a spatial path.*

**INTRODUCTION**

Spatial path tracking requires that the controlled point on the end-effector (EE) of a manipulator follow a prescribed spatial curve. Typically, the task is accomplished by obtaining the instantaneous time-based first- and second-order properties, i.e. ve-

locities and accelerations, of the mechanism's joints via Jacobian inversion [1]. For planar cases, an alternative approach, developed in [2], separates the control of the path variable from the control of the output-space trajectory geometry via curvature theory, providing a time-invariant means of path tracking. Time invariance implies the ability to track the output-space path geometry independent of the EE speed. There are no kinematic singularities in the control of the output-trajectory geometry; they occur only in the control of the path variable which experiences a dwell in its trajectory [2]. Therefore, a major advantage of this method is that it achieves faithful tracking of the output-path geometry for singular mechanism poses. Further, the time-invariant solution allows the tracking of the desired EE path at any desired, feasible speed. This characteristic could be useful in an industrial setting where repetitive operations, such as pick-and-place, need to be executed at different speeds. This method uses only local path information that can be gathered using a vision feedback system to execute tracking [3], making the approach more adaptable to external disturbances. The method also reduces the reliance of the tracking performance on accurate system calibration since the processes of error sensing and path correction take place in the output space.

A  $q^{th}$ -order geometric path-tracking task requires the instantaneous  $q^{th}$ -order geometric properties of the motion of the controlled point,  $P$ , on the EE to be identical to the instantaneous  $q^{th}$ -order geometric properties of the desired curve. The kinematic equations of motion of point  $P$  in the general form are

\*Address all correspondence to this author.

obtained by considering  $P$  to be an arbitrary point in a moving reference frame and expressing its motion with respect to a fixed reference frame. The motion is expressed as a function of two independent motion parameters for planar motion, and three independent parameters for spatial motion. The existing approach to planar geometric path tracking in [2] starts by generalizing the planar 2-degree-of-freedom (DOF) curvature theory [4] to arbitrary DOFs and parsimoniously expresses the motion of  $P$  as a function of two arbitrary motion parameters in a canonical reference frame. The kinematic equations of motion of  $P$  are obtained by writing the position vector for  $P$  and differentiating it with respect to the motion parameters. When a particular two-DOF mechanism is prescribed for the tracking task, the forward kinematics of the mechanism give the position vector of point  $P$ , and the joint displacements are conveniently chosen as the motion parameters. To obtain equivalence between the desired path, a single-DOF object, and the motion of  $P$ , as yet a two-DOF object, the instantaneous motions of the two joints are constrained using a Taylor series, the constants of which are called speed ratios. The motion of  $P$  is now function of a single joint variable, and the instantaneous geometric properties of the path of  $P$  up to order  $q$  are forced to be identical to the corresponding properties of the desired curve by appropriately choosing the speed ratios up to the  $q^{\text{th}}$  order. Thus, obtaining expressions for the speed ratios as functions of the geometric properties of the desired path and the mechanism's current pose is the key to geometric path tracking.

Most work relating to geometric tracking has been limited to planar, non-redundant tracking systems. General expressions for the first- and second-order speed ratios using second-order information (tangent direction and curvature) of the output path and the instantaneous invariants of motion have been developed in [2]. Instantaneous invariants are geometric quantities that naturally occur while obtaining the kinematic equations of motion [4, 5]. Particular expressions for the ratios for specific mechanisms such as a planar revolute-revolute (RR) system and a non-holonomic cart system are also provided in [2], and particular expressions for a planar prismatic-revolute positioner are given in [6]. The general expression for the third-order ratio for a planar system tracking constant-curvature paths, and particular expression for a RR system are developed in [7]. Means to obtain higher-order speed ratios for planar system tracking an arbitrary path have not been developed.

Extension of the planar formulation [2] to second-order path tracking using spatial, non-redundant systems that include a planar two-DOF subsystem was achieved by [8]. As an example, this work provides particular expressions for the first- and second-order speed ratios of the regional structure (i.e. manipulators used only for translating the EE) of the Stanford Arm (a rotating RP mechanism). This technique, though, cannot be extended to arbitrary three-DOF spatial regional systems. Further, methods to obtain third- and higher-order speed ratios for any

spatial regional mechanism do not exist.

The technique described in this paper differs from previous methods in three ways. First, since a single-parameter representation of the EE motion is required for geometric path-tracking, the position vector of the EE is represented as a function of a *single* joint variable. Higher-order kinematic equations of motion are then obtained by differentiating the position vector with respect to the *single* joint variable. Secondly, the Frenet-Serret (FS) framework is used to describe the differentiated vector as well as the geometric properties of the desired path. Finally, this development can be carried out in any convenient reference frame, and a fixed reference frame is used in this paper in contrast to the canonical frame used in previous methods. This is a significant advantage since the canonical frame, although it provides parsimony of expression, is a pose-dependent, moving frame and therefore, unsuitable for the implementation of path-tracking. Here, parsimony of expression is not sought. Rather, the focus is on describing the kinematics to any order. This approach has allowed the development of a novel methodology for finding the speed ratios of any order, and even though the expressions of the differentiated position vector can get complicated, the resulting equations of motion are shown to be always linear in the speed ratios.

The formulation in this paper has the potential to shed light on the tracking capabilities of spatial mechanisms in singular poses. It is known that, for planar mechanisms in singular poses, it is possible to track the geometry of the output path, but the control of the output-space trajectory geometry is degraded [2]. The study of the tracking capabilities of spatial mechanisms in first- and second-order singular poses is a subject of future work, but it can be shown that it is usually possible to track the desired trajectory tangent when the spatial mechanism is in a singular pose. This is not possible with time-based approaches to path tracking, wherein only the feasible component of the commanded output-space velocity is tracked at a singularity [9]. Thus, superior geometric tracking accuracy near and at singular poses is a significant advantage of geometric path tracking.

An alternative way of obtaining the speed ratios using time-based joint motions is also described in this paper. The  $q^{\text{th}}$ -order speed ratios can be obtained from the  $q^{\text{th}}$ -order, time-based joint motions which, in turn, can be obtained by inverting the  $q^{\text{th}}$ -order, three-DOF forward-kinematic equation of motion. [10] provide the canonical system, the forward kinematic equations of motion, and the instantaneous invariants for spatial motion with up to five DOF. Therefore, the canonical three-DOF motion equation can be used to obtain parsimonious expressions for the speed ratios. However, the use of the canonical system is unsuitable for the present application. Also, for singular mechanism poses, this method is not useful since the time-based joint motions cannot be obtained.

The spatial 3-revolute (3R) open chain is used to illustrate the application of the techniques developed here. The instan-

taneous kinematics of this mechanism have been studied extensively. For example, the inverse velocity and acceleration solutions for the mechanism are given in [11], and expressions for the angular velocity, the pitch, and the instantaneous screw axis of the EE as functions of the first-order speed ratios are obtained in [12]. Geometric path tracking with the mechanism, though, has not been done. Also, the 3R chain has been chosen here because of its morphological similarity to the human arm and the possible application of the ideas in this paper to human motor-control of arm motions. It has been observed [13] that the wrist path during reaching motions to a given target are speed invariant. It has been proposed that the time-invariant approach outlined herein may describe how the human central nervous system achieves such behavior [14].

The rest of the paper is organized as follows. The next section outlines the methodology to obtain the speed ratios of any order via the derivation of the ratios up to order 3. Some special cases are also discussed here. The following section addresses some implementation issues and methods to reduce tracking error. The next section applies the results to obtain the speed ratios of a spatial 3R mechanism and uses them to track a helical path. Finally, conclusions are given.

## PATH TRACKING VIA JOINT COORDINATION

### Notation:

A trailing subscript(s) indicates partial derivative with respect to the subscript(s). For example,  $\bar{r}_\lambda := \frac{d\bar{r}}{d\lambda}$ . A zero after the subscript(s) indicates that the derivative has been evaluated in the zero position. For example,  $\bar{r}_{\lambda\mu 0} := \frac{\partial^2 \bar{r}}{\partial \lambda \partial \mu} \Big|_0$ . The dot notation indicates derivatives with respect to time  $t$ . For example,  $\dot{\lambda} := \frac{d\lambda}{dt} \Big|_0$ . The symbols  $n$  and  $k$  always represent the speed ratios with respect to a leading joint variable. A trailing superscript indicates the order of the ratio. For example,  $k^{(3)} := \frac{d^3 v}{d\lambda^3} \Big|_0$ . The superscript is omitted for the first-order ratios, so  $n^{(1)} := n$ .

The *desired path* is a spatial curve  $\bar{R}(s)$ , parameterized in terms of its arc length  $s$ . A general non-redundant manipulator capable of tracking a spatial curve must have three DOF, the joint variables of which may be denoted as  $v$ ,  $\lambda$  and  $\mu$ . Without loss of generality, the instantaneous values of  $v$ ,  $\lambda$  and  $\mu$  are taken to be zero, which defines the zero position. In the zero position, the values of the joint variables are denoted by  $v_0$ ,  $\lambda_0$ , and  $\mu_0$  instead of the standard Denavit-Hartenberg (DH) parameters  $\theta_1$ ,  $\theta_2$ , and  $\theta_3$ , respectively, to maintain consistency with previous literature pertaining to geometric tracking [2, 4, 6, 7]. In the zero position, the path traced by the position vector of the EE, called the *generated path*  $\bar{r}$ , must have the same instantaneous geometric properties as the desired path. The order to which the geometric properties are matched determines the order of joint coordination, or vice-versa. For example, first-order joint coordination is required to match the first-order property, i.e. tangent direc-

tion, while second-order joint coordination matches the tangent direction and the center of curvature.

The desired path is described in terms of the natural trihedron of the FS frame [15]. The natural trihedron has a unit tangent vector  $\hat{T}$ , unit principal normal  $\hat{N}$ , and binormal  $\hat{B} = \hat{T} \times \hat{N}$ . The FS formulas relate the trihedral vectors to their rates of change with respect to the arc length. In matrix form [16],

$$\begin{bmatrix} \frac{d\hat{T}}{ds} \\ \frac{d\hat{N}}{ds} \\ \frac{d\hat{B}}{ds} \end{bmatrix} = \begin{bmatrix} 0 & \kappa & 0 \\ -\kappa & 0 & \tau \\ 0 & -\tau & 0 \end{bmatrix} \begin{bmatrix} \hat{T} \\ \hat{N} \\ \hat{B} \end{bmatrix}, \quad (1)$$

where  $s = 0$  at the zero position,  $\kappa$  is the curvature, and  $\tau$  is the torsion of the spatial curve. Note that the third-order geometric property  $\tau$  appears in Eqn. (1). Therefore, third-order joint coordination is required to fully match the FS description of the desired path with the generated path. Higher orders of coordination match the derivatives of  $\kappa$  and  $\tau$ .

A natural parameterization of the generated path is achieved via the mechanism's forward kinematics in terms of the mechanism's joint variables:  $\bar{r} = \bar{r}(v, \lambda, \mu)$ . The joint motions are coordinated so that the mechanism effectively has a single DOF. Arbitrarily choosing  $\lambda$  as the independent variable or *leading joint*, the joint-coordination equations are

$$\begin{aligned} \mu &= n\lambda + \frac{n^{(2)}}{2}\lambda^2 + \frac{n^{(3)}}{6}\lambda^3 + \dots, \\ v &= k\lambda + \frac{k^{(2)}}{2}\lambda^2 + \frac{k^{(3)}}{6}\lambda^3 + \dots, \end{aligned} \quad (2)$$

where the speed ratios are defined as

$$\begin{aligned} n &:= \frac{d\mu}{d\lambda} \Big|_0, n^{(2)} := \frac{d^2\mu}{d\lambda^2} \Big|_0, n^{(3)} := \frac{d^3\mu}{d\lambda^3} \Big|_0, \dots, \\ k &:= \frac{dv}{d\lambda} \Big|_0, k^{(2)} := \frac{d^2v}{d\lambda^2} \Big|_0, k^{(3)} := \frac{d^3v}{d\lambda^3} \Big|_0, \dots \end{aligned}$$

There are two ratios for every order of coordination. Although  $\lambda$  is arbitrarily chosen as the leading joint variable for developing the arguments in this paper, the choice merits some discussion. A leading joint must provide finite speed ratios for any desired order of coordination. A sufficient condition for this is that the leading joint should have non-zero, finite velocity, i.e. it should not be at a dwell. This issue is discussed in detail in [17]. Choosing the leading joint allows for the parameterization  $\bar{r} = \bar{r}(\lambda)$ . Therefore, the Taylor series expansion of  $\bar{r}$  at the zero position

can be written as

$$\begin{aligned}\bar{r}(\lambda) &= \bar{r}_0 + \lambda \left. \frac{d\bar{r}}{d\lambda} \right|_0 + \frac{\lambda^2}{2} \left. \frac{d^2\bar{r}}{d\lambda^2} \right|_0 + \frac{\lambda^3}{6} \left. \frac{d^3\bar{r}}{d\lambda^3} \right|_0 + \dots \\ &= \bar{r}_0 + \lambda \bar{r}_{\lambda 0} + \frac{\lambda^2}{2} \bar{r}_{\lambda\lambda 0} + \frac{\lambda^3}{6} \bar{r}_{\lambda\lambda\lambda 0} + \dots\end{aligned}\quad (3)$$

Note that  $\bar{r}_0$  is the current pose of the mechanism. Also,  $\bar{r}_{\lambda 0} = \bar{r}_{\lambda 0}(n, k)$ ,  $\bar{r}_{\lambda\lambda 0} = \bar{r}_{\lambda\lambda 0}(n, k, n^{(2)}, k^{(2)})$ , and so on. The desired order of joint coordination defines the order at which the Taylor series in Eqn. (2) and Eqn. (3) are terminated. For non-singular poses, the order of joint coordination corresponds to the order to which the geometric properties of the desired and the generated paths are matched. Discussion of the case when the mechanism's pose is singular is a subject of future work.

The order of coordination proceeds in stages from the zeroth to the third and higher orders. At each order of coordination, it is assumed that all lower orders of coordination have been achieved. For each order of coordination except the zeroth order, a vector equation involving two unknown speed ratios, called *the coordination equation*, is obtained. The coordination equation is used to obtain the two speed ratios as discussed below.

### Zeroth-order Coordination

This involves achieving the appropriate pose of the mechanism by solving the inverse position kinematics problem. In the foregoing, it is assumed that the EE is on the desired path in the zero position. This is a reasonable assumption to make, since the problem of path tracking mainly involves considerations of derivatives of the position, rather than of position itself. Therefore, rather than explicitly solve the inverse position kinematics problem, it is considered solved by virtue of the current pose of the mechanism.

### First-order Coordination

The desired tangent direction is achieved by first-order coordination. From differential geometry,

$$\begin{aligned}\hat{T} &= \bar{r}_{s0} = \bar{r}_{\lambda 0} / s_{\lambda 0}, \\ \Rightarrow \bar{r}_{\lambda 0} &= s_{\lambda 0} \hat{T}.\end{aligned}\quad (4)$$

Cross multiplying by  $\hat{T}$  gives

$$\bar{r}_{\lambda 0} \times \hat{T} = \bar{0}.\quad (5)$$

Equation (5) is the first-order coordination equation, which simply states that the vectors  $\bar{r}_{\lambda 0}$  and  $\hat{T}$  are parallel. It can be solved for the first-order ratios  $n$  and  $k$ .

### Second-order Coordination

Differentiating Eqn. (4) with respect to the leading joint variable  $\lambda$  and using Eqn. (1) gives

$$\bar{r}_{\lambda\lambda 0} = s_{\lambda\lambda 0} \hat{T} + (s_{\lambda 0})^2 \kappa \hat{N}.\quad (6)$$

From differential geometry,

$$\begin{aligned}s_{\lambda 0} &= \sqrt{\bar{r}_{\lambda 0} \cdot \bar{r}_{\lambda 0}}, \\ \therefore s_{\lambda\lambda 0} &= \bar{r}_{\lambda\lambda 0} \cdot \hat{r}_{\lambda 0} = \bar{r}_{\lambda\lambda 0} \cdot \hat{T}.\end{aligned}\quad (7)$$

Substituting Eqn. (7) into Eqn. (6) gives

$$\bar{r}_{\lambda\lambda 0} = (\bar{r}_{\lambda\lambda 0} \cdot \hat{T}) \hat{T} + \kappa (\bar{r}_{\lambda 0} \cdot \bar{r}_{\lambda 0}) \hat{N}.$$

Cross multiplying by  $\hat{T}$  and using  $\hat{T} \times \hat{N} = \hat{B}$  gives

$$\bar{r}_{\lambda\lambda 0} \times \hat{T} + \kappa (\bar{r}_{\lambda 0} \cdot \bar{r}_{\lambda 0}) \hat{B} = \bar{0}.\quad (8)$$

Equation (8) is the second-order coordination equation. It is used to obtain the second-order ratios  $n^{(2)}$  and  $k^{(2)}$ .

### Third-order Coordination

Differentiating Eqn. (8) gives the third-order coordination equation,

$$\begin{aligned}\bar{r}_{\lambda\lambda\lambda 0} \times \hat{T} - \kappa \tau (\bar{r}_{\lambda 0} \cdot \bar{r}_{\lambda 0})^{\frac{3}{2}} \hat{N} + \\ \left[ \kappa_{s0} (\bar{r}_{\lambda 0} \cdot \bar{r}_{\lambda 0})^{\frac{3}{2}} + 3\kappa (\bar{r}_{\lambda 0} \cdot \bar{r}_{\lambda\lambda 0}) \right] \hat{B} = \bar{0}.\end{aligned}\quad (9)$$

Equation (9) is the third-order coordination equation, and it can be used to solve for the third-order speed ratios  $n^{(3)}$  and  $k^{(3)}$ .

### Higher-order Coordination

In general, if the desired path is regular ( $p$ -times differentiable), the procedure outlined above can be continued to the  $p^{th}$  order. Equation (4) can be differentiated repeatedly, with each successive differentiation generating two speed ratios. The ratios can be obtained from the corresponding coordination equation of the type seen in Eqn. (5), Eqn. (8), and Eqn. (9). Once all the speed ratios are obtained, Eqn. (3) is used to generate the path of the EE as a function of the leading variable  $\lambda$ .

The coordination equations can be described using the following general form. The  $p^{th}$ -order coordination equation states that the cross product of the tangent direction with the

$p^{th}$ -derivative of  $\bar{r}$  evaluated at the zero position is a known quantity. Therefore,

$$\bar{r}_{(\lambda\lambda\dots p \text{ times})0} \times \hat{T} + \bar{X} = \bar{0}, \quad (10)$$

where the known quantity  $\bar{X}$  is a function of the derivatives of the kinematic map up to and including the order  $p - 1$  and the geometric properties of the desired path. Therefore, for the  $p^{th}$ -order coordination equation, only the term  $\bar{r}_{(\lambda\lambda\dots p \text{ times})0} \times \hat{T}$  will contain the  $p^{th}$ -order speed ratios. Note that Eqn. (10) has a structure similar to that of the higher-order time derivative of the function  $\bar{r}(v, \lambda, \mu)$ :

$$\begin{aligned} \dot{\bar{r}} &= J\dot{\bar{\theta}}, \\ \ddot{\bar{r}} &= J\ddot{\bar{\theta}} + \left[ \dot{J}\dot{\bar{\theta}} \right], \\ \ddot{\bar{r}} &= J\ddot{\bar{\theta}} + \left[ 2\dot{J}\dot{\bar{\theta}} + J\ddot{\bar{\theta}} \right], \dots \end{aligned} \quad (11)$$

where  $J$  is the Jacobian of  $\bar{r}(v, \lambda, \mu)$ ,  $\bar{\theta} = [v \ \lambda \ \mu]^T$ , and the bracketed quantities are known. Clearly, each of the equations in Eqn. (11) is linear in the highest-order joint variable motion. This linear structure is not lost in the present reparametrization of the motion, and Appendix 1 shows that the leading term in Eqn. (10) is linear in the  $p^{th}$ -order speed ratios, which is a crucial advantage from the computational point of view. Further, the coordination equation of any order generates three component equations with two unknown speed ratios. Appendix 1 also shows that the component equations are always consistent<sup>1</sup>.

### Speed Ratios from Time-Based Joint Motions

When the  $p^{th}$ -order time-based solution for the joint motions exists, an alternative way to obtain the speed ratios is by differentiating the Taylor series in Eqn. (2) with respect to time  $t$ . The differentiation can be carried out using Faa di Bruno's formula [18, 19] for the  $p^{th}$ -order differentiation of composite functions. For example, the  $p^{th}$ -order differentiation of the composite function  $\mu(\lambda(t))$  with respect to  $t$  is given by

$$\frac{d^p \mu}{dt^p} = \sum \frac{p!}{g_1! \dots g_p!} \cdot \frac{d^g \mu}{d\lambda^g} \cdot \left( \frac{d\lambda/dt}{1!} \right)^{g_1} \dots \left( \frac{d^p \lambda/dt^p}{p!} \right)^{g_p}, \quad (12)$$

where the sum is over all different solutions in nonnegative integers  $g_1, \dots, g_p$  of  $g_1 + 2g_2 + \dots + pg_p = p$ , and  $g := g_1 + \dots + g_p$ .

<sup>1</sup>This is true as long as the manipulator is in a non-singular pose, i.e. the Jacobian in Eqn. (11) is full rank.

Note that  $g \leq p$ . Further, in the zero position, the term  $\frac{d^g \mu}{d\lambda^g}$  is the  $g^{th}$ -order speed ratio. Also, for  $g = p$ ,

$$\begin{aligned} g_1 + g_2 + \dots + g_p &= p, \\ g_1 + 2g_2 + \dots + pg_p &= p, \\ \Rightarrow g_2 + 2g_3 + \dots + (p-1)g_p &= 0, \\ \Rightarrow g_i = 0, \text{ for } i = 2, 3, \dots, p, \text{ and } g_1 &= p. \end{aligned}$$

Therefore, for  $g = p$ , the sum in Eqn. (12) reduces to  $n^{(p)}(\dot{\lambda})^p$  in the zero position. Equation (12) can now be written as

$$\begin{aligned} \frac{d^p \mu}{dt^p} \Big|_0 &= \sum \frac{p!}{g_1! \dots g_p!} \cdot n^{(g)} \cdot \left( \frac{d\lambda/dt}{1!} \right)^{g_1} \dots \\ &\quad \left( \frac{d^p \lambda/dt^p}{p!} \right)^{g_p} + n^{(p)}(\dot{\lambda})^p, \\ \Rightarrow n^{(p)} &= \frac{1}{(\dot{\lambda})^p} \cdot \left\{ \frac{d^p \mu}{dt^p} \Big|_0 - \sum \frac{p!}{g_1! \dots g_p!} \cdot n^{(g)} \cdot \right. \\ &\quad \left. \left( \frac{d\lambda/dt}{1!} \right)^{g_1} \dots \left( \frac{d^p \lambda/dt^p}{p!} \right)^{g_p} \right\}, \end{aligned} \quad (13)$$

where  $g \leq p - 1$ . Equation (13) obtains the  $p^{th}$ -order ratio as a function of the previous  $p - 1$  ratios and the time derivatives of the joint variables up to the  $p^{th}$ -order.

The time-based and the time-independent methods of finding the speed ratios given in this section are equivalent, although the later provides geometric insight into the process of path tracking.

### Special Cases

This section addresses two special cases of the FS parameterization of the output-space curve.

**Tracking Straight Lines** If the desired path is a straight line, the following conditions hold:  $\kappa = 0, \tau = 0$ , and all derivatives of  $\kappa$  and  $\tau$  with respect to  $s$  are zero. Also,  $\hat{N}$  and  $\hat{B}$  are not uniquely defined. As a result, Eqn. (5), Eqn. (8), and Eqn. (9) reduce to

$$\bar{r}_{\lambda 0} \times \hat{T} = \bar{0}, \quad (14)$$

$$\bar{r}_{\lambda \lambda 0} \times \hat{T} = \bar{0}, \quad \text{and} \quad (15)$$

$$\bar{r}_{\lambda \lambda \lambda 0} \times \hat{T} = \bar{0}. \quad (16)$$

Equations (14), (15), and (16) can be solved to obtain the speed ratios up to the third order. In fact, the  $p^{th}$ -order coordination equation is

$$\bar{r}_{(\lambda\lambda\dots p \text{ times})0} \times \hat{T} = \bar{0}.$$

**Inflection Points on the Desired Path** The FS parameterization has a singularity at an inflection point ( $\kappa = 0$ ) because a unique principal normal cannot be determined. This difficulty can be resolved by using limit analysis as demonstrated in [20]. Here, the curvature of the desired path  $\bar{R}$  is approximated by a linear function of the arc length in the vicinity of the inflection point. The function is substituted into the expression for the normal vector  $\hat{N} = \frac{\bar{R}_{ss0}}{\kappa(s)}$ . The limit, obtained via use of de l'Hôpital's rule, gives the principal normal (for  $|\bar{R}_{sss0}| \neq 0$ ). The first- and second-order coordination equations for this case are the same as Eqn. (14) and Eqn. (15), respectively. The third-order coordination equation is

$$\bar{r}_{\lambda\lambda\lambda} \times \hat{T} + \kappa_{s0} (\bar{r}_{\lambda 0} \cdot \bar{r}_{\lambda 0})^{\frac{3}{2}} \hat{B} = \bar{0}.$$

## IMPLEMENTATION ISSUES

The Taylor series relating the motion of the mechanism's joints is valid instantaneously. As the mechanism moves from its zero position, the controlled point on the EE moves away from the desired path, thus creating error in the tracking. Although the rate of increase in error with respect to the leading-joint motion is significantly lower for higher orders of joint coordination, it cannot be eliminated. Therefore, some mechanism for intermittent correction is essential for controlling the accumulating error away from the zero position. Corrective algorithms using error sensing in the output space have been suggested for planar path tracking [21] and for spatial systems [17]. Here, the system senses the position error, which is the minimum distance between the desired path and the current position of the controlled point. Corrective action is taken if a predefined error limit is exceeded. The corrective action involves locally defining a new desired path such that further motion of the mechanism reduces the position error. Although [21] and [17] demonstrate the feasibility of such a corrective algorithm, how to optimally define the new desired path and ensure stability remain open questions.

## ILLUSTRATIVE EXAMPLE

The spatial 3R mechanism shown in Fig. 1 is used here to illustrate the path-tracking approach outlined in this paper. This system is in fact a three-DOF system with a planar subsystem and of the kind investigated in [8]. The mechanism has two revolute joints whose axes intersect orthogonally at point  $A^*$  and a third revolute joint whose axis passes through point  $A$  and is parallel to the distal interior joint axis. The fixed coordinate frame is placed at  $A^*$  with the  $Z$  axis oriented along the joint axis denoted by joint angle  $v$ . The DH parameters for this mechanism geometry are  $a_1 = 0, \alpha_1 = \frac{\pi}{2}, \alpha_2 = 0, \alpha_3 = 0, d_2 = 0,$  and  $d_3 = 0$ . With the origin of the reference frame at point  $A^*$  the parameter  $d_1 = 0$ . The joint angles of the revolute joints are denoted

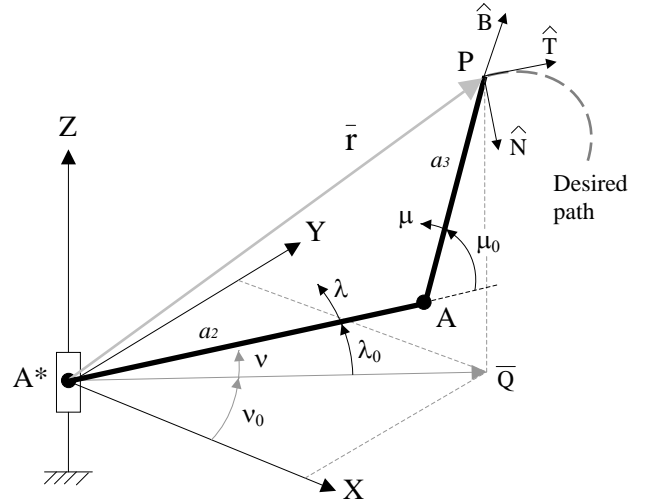


Figure 1. THE SPATIAL 3R MECHANISM IS REQUIRED TO TRACK THE DESIRED PATH. THE VECTORS  $\hat{T}$ ,  $\hat{N}$ , AND  $\hat{B}$  FORM THE TRIHEDRON OF THE FS FRAME AND DESCRIBE THE PATH GEOMETRY. THE GEOMETRY IS TRACKED BY RELATING THE MOTIONS OF JOINT VARIABLES  $\mu$  AND  $v$  TO THAT OF JOINT VARIABLE  $\lambda$ .

by  $\theta_1 = v_0, \theta_2 = \lambda_0,$  and  $\theta_3 = \mu_0,$  defining the current pose and the zero position of the mechanism, wherein the speed ratios are calculated. The increments in these angles are  $v, \lambda,$  and  $\mu,$  respectively, which are all zero in the zero position.

The desired path is shown in Fig. 1. The EE, denoted by point  $P$ , is assumed to be on the desired path in the zero position. The natural trihedron of the desired path at point  $P$  is the unit tangent  $\hat{T}$ , the unit normal  $\hat{N}$ , and the binormal  $\hat{B}$ . The curvature  $\kappa$ , torsion  $\tau$ , and quantity  $\kappa_{s0}$  are not shown in the figure.

For the purpose of obtaining the speed ratios,  $\lambda$  is chosen as the leading joint angle. The position vector  $\bar{r}$  of the EE is expressed using the forward kinematics of the mechanism as a function of  $\lambda$  as

$$\bar{r}(\lambda) = \begin{bmatrix} a_2 C_{\lambda_0 + \lambda} C_{v_0 + v(\lambda)} + a_3 C_{\psi} C_{v_0 + v(\lambda)} \\ a_2 C_{\lambda_0 + \lambda} S_{v_0 + v(\lambda)} + a_3 C_{\psi} S_{v_0 + v(\lambda)} \\ a_2 S_{\lambda_0 + \lambda} + a_3 S_{\psi} \end{bmatrix}, \quad (17)$$

where  $a_2$  and  $a_3$  are the link lengths,  $\psi = \lambda_0 + \mu_0 + \lambda + \mu(\lambda),$  and the functions  $\mu(\lambda)$  and  $v(\lambda)$  are the Taylor series given by Eqn. (2). 'C' and 'S' denote the *cos* and *sine* functions for the remainder of the paper. The derivatives of  $\mu$  and  $v$  with respect to the leading joint variable  $\lambda$ , evaluated in the zero position, are the speed ratios of the mechanism, as defined in Eqn. (3).

For third-order coordination, Eqn. (17) is differentiated with

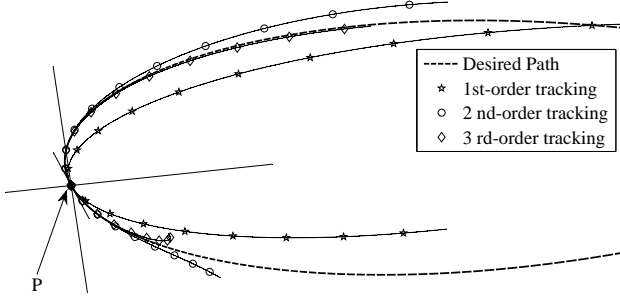


Figure 2. THE PATHS TRACED BY POINT  $P$  ON THE EE OF THE 3R MECHANISM FOR FIRST-, SECOND-, AND THIRD-ORDER JOINT COORDINATION ARE SHOWN. HIGHER ORDER OF JOINT COORDINATION RESULTS IN  $P$  FOLLOWING THE DESIRED PATH MORE CLOSELY NEAR THE ZERO POSITION.

respect to the leading joint variable  $\lambda$  three times to give

$$\bar{r}_{\lambda 0} = \begin{bmatrix} -a_2 S_{\lambda_0} C_{\psi_0} - a_2 k C_{\lambda_0} S_{\psi_0} \\ -a_3 (1+n) S_{\psi_0} C_{\psi_0} - a_3 k C_{\psi_0} S_{\psi_0} \\ -a_2 S_{\lambda_0} S_{\psi_0} + a_2 k C_{\lambda_0} C_{\psi_0} \\ -a_3 (1+n) S_{\psi_0} S_{\psi_0} + a_3 k C_{\psi_0} C_{\psi_0} \\ a_2 C_{\lambda_0} + a_3 (1+n) C_{\psi_0} \end{bmatrix}, \quad (18)$$

$$\bar{r}_{\lambda \lambda 0} = \bar{A} + n^{(2)} \bar{D} + k^{(2)} \bar{H}, \quad (19)$$

$$\bar{r}_{\lambda \lambda \lambda 0} = \left( \bar{A}_\lambda + n^{(2)} \bar{D}_\lambda + k^{(2)} \bar{H}_\lambda \right) + n^{(3)} \bar{D} + k^{(3)} \bar{H}, \quad (20)$$

where  $\psi_0 = \lambda_0 + \mu_0$ , and the components of the vectors  $\bar{A}$ ,  $\bar{D}$ , and  $\bar{H}$  are functions of the current pose, link lengths and the ratios  $n$  and  $k$ , and the components of the vectors  $\bar{A}_\lambda$ ,  $\bar{D}_\lambda$ , and  $\bar{H}_\lambda$  are functions of the current pose, link lengths, and ratios  $n$ ,  $k$ ,  $n^{(2)}$ , and  $k^{(2)}$ . These functions are given in Appendix 2.

Equation (18) is substituted into Eqn. (5) to get the first-order speed ratios

$$n = -\frac{a_2 [T(1)C_{\psi_0}C_{\lambda_0} + T(2)S_{\psi_0}C_{\lambda_0} + T(3)S_{\lambda_0}]}{a_3 [T(1)C_{\psi_0}C_{\psi_0} + T(2)S_{\psi_0}C_{\psi_0} + T(3)S_{\psi_0}]} - 1,$$

and

$$k = \frac{a_2 S_{\mu_0} [T(2)C_{\psi_0} - T(1)S_{\psi_0}]}{|\bar{Q}| [T(1)C_{\psi_0}C_{\psi_0} + T(2)S_{\psi_0}C_{\psi_0} + T(3)S_{\psi_0}]},$$

where  $\bar{Q}$  is the projection of the position vector  $\bar{r}$  onto the  $XY$  plane as shown in Fig. 1 such that  $|\bar{Q}| = a_2 C_{\lambda_0} + a_3 C_{\psi_0}$ .

Substituting Eqn. (19) into Eqn. (8) and Eqn. (20) into Eqn. (9) gives

$$\begin{bmatrix} \bar{D} \times \hat{T} & \bar{H} \times \hat{T} \end{bmatrix} \begin{bmatrix} n^{(2)} \\ k^{(2)} \end{bmatrix} = \bar{\Psi}_1, \quad (21)$$

$$\begin{bmatrix} \bar{D} \times \hat{T} & \bar{H} \times \hat{T} \end{bmatrix} \begin{bmatrix} n^{(3)} \\ k^{(3)} \end{bmatrix} = \bar{\Psi}_2, \quad (22)$$

where,

$$\bar{\Psi}_1 = -\bar{A} \times \hat{T} - \kappa (\bar{r}_{\lambda 0} \cdot \bar{r}_{\lambda 0}) \hat{B},$$

$$\begin{aligned} \bar{\Psi}_2 = & -(\bar{A}_\lambda + n^{(2)} \bar{D}_\lambda + k^{(2)} \bar{H}_\lambda) \times \hat{T} \\ & + \kappa \tau (\bar{r}_{\lambda 0} \cdot \bar{r}_{\lambda 0})^{\frac{3}{2}} \hat{N} - \left[ \kappa_{s0} (\bar{r}_{\lambda 0} \cdot \bar{r}_{\lambda 0})^{\frac{3}{2}} \right. \\ & \left. + 3\kappa (\bar{r}_{\lambda 0} \cdot \bar{r}_{\lambda 0}) \right] \hat{B}. \end{aligned}$$

Note that  $\bar{\Psi}_1$  and  $\bar{\Psi}_2$  are known quantities. Any two equations from Eqn. (21) can be solved for the ratios  $n^{(2)}$  and  $k^{(2)}$ , and likewise, any two equations from Eqn. (22) can be solved for the third-order ratios  $n^{(3)}$  and  $k^{(3)}$ . Appendix 1 shows that the component equations of Eqn. (21) and Eqn. (22) are always consistent.

These results are illustrated by means of a particular tracking task. The mechanism is defined with link lengths  $a_2 = 1$  and  $a_3 = 1.5$  and initial pose  $\nu_0 = 40^\circ$ ,  $\mu_0 = 70^\circ$ , and  $\lambda_0 = 10^\circ$ . Note that any unit of length for  $a_2$  and  $a_3$  will be appropriate. The desired path is a helix given in terms of its arc length  $s$  as

$$\bar{R}(s) = \left[ \cos\left(\frac{s}{\sqrt{2}}\right) + 1 \quad \sin\left(\frac{s}{\sqrt{2}}\right) \quad \frac{s}{\sqrt{2}} \right]^T + \bar{r}_0, \quad (23)$$

where  $\bar{r}_0$  is the current position of point  $P$ . Equation (23) ensures that  $P$  is on the desired path at the zero position. The curvature  $\kappa = \frac{1}{2}$ , the torsion  $\tau = \frac{1}{2}$ , and  $\kappa_{s0} = 0$ . Also,  $\hat{T} = [0 \quad \frac{1}{\sqrt{2}} \quad \frac{1}{\sqrt{2}}]^T$ ,  $\hat{N} = [-1 \quad 0 \quad 0]^T$ , and  $\hat{B} = [0 \quad -\frac{1}{\sqrt{2}} \quad \frac{1}{\sqrt{2}}]^T$ . The speed ratios are,

$$\begin{aligned} n &= -1.4905, & n^{(2)} &= -0.2985, & n^{(3)} &= 0.3481, \\ k &= 0.5272, & k^{(2)} &= -0.4606, & k^{(3)} &= -0.5945. \end{aligned}$$

Note that the first- and second-order speed ratios could also be obtained using Eqn. (13) and the inverse velocity and acceleration solutions given by [11] since the mechanism is not in a singular pose.

Figure 2 shows the desired helical path and the tracking results for the first, second, and third orders. The generated paths are plotted for  $\lambda = 0$  (zero position) to  $\lambda = +50^\circ$  and  $\lambda = -60^\circ$ .

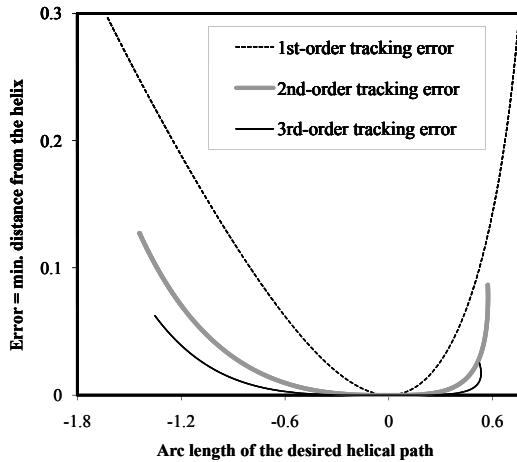


Figure 3. TRACKING ERROR IS THE MINIMUM DISTANCE OF  $P$  FROM THE DESIRED PATH. ERROR INCREASES AS  $P$  MOVES AWAY FROM THE ZERO POSITION. HIGHER ORDER JOINT COORDINATION RESULTS IN LOWER ERROR NEAR THE ZERO POSITION.

The cross-hairs intersecting at point  $P$  indicate the natural trihedron of the helix. Figure 3 plots the tracking error against the arc length of the helix for the three tracking results. The error is defined as the minimum distance between the current position of  $P$  and the desired helical path. Error is calculated after every  $10^{-3}$ -degree increment in  $\lambda$ . Figure 3 clearly shows that near the zero position  $s = 0$ , a higher order of coordination results in significantly lower position error.

## CONCLUSIONS

This paper presents a novel method for finding the speed ratios of any order of any spatial or planar non-redundant regional mechanism using a fixed coordinate frame. The Frenet-Serret parameterization is used to describe the desired path. Repeated differentiation of the forward kinematic map of the mechanism provides a description of the generated path, and its comparison to the desired path generates coordination equations that are linear in the speed ratios. A 3R spatial mechanism is used to illustrate the technique. A numerical example is presented wherein the 3R mechanism tracks a desired helical path using first-, second- and third-order joint coordination. Higher order joint coordination results in significantly lower position error near the zero position.

## ACKNOWLEDGMENT

The authors would like to thank Mr. Udayan Kanade of Oneirix Labs, Pune, for his input on obtaining speed ratios from time-based joint motions.

## REFERENCES

- [1] Waldron, K. J., and Schmiedeler, J. P., 2008. "Kinematics". In *Springer Handbook of Robotics*, B. Siciliano and O. Khatib, eds. Springer Verlag, Western Europe, Chapter 1, pp. 9–33.
- [2] Lorenc, S. J., Stanisic, M. M., and Hall, A. S. J., 1995. "Application of Instantaneous Invariants to the Path Tracking Control Problem of Planar Two Degree-of-Freedom Systems: A Singularity-Free Mapping of Trajectory Geometry". *Mechanism and Machine Theory*, **30**(6), August, pp. 883–896.
- [3] Nesnas, I. A. D., and Stanisic, M. M., 1994. "Robotics Software Development Using Object-Oriented Design". In *ASME Design Automation Conference*, A. Editor and B. Editor, eds., Vol. 69, pp. 83–92.
- [4] Bottema, O., and Roth, B., 1979. *Theoretical Kinematics*. North Holland, Amsterdam.
- [5] Roth, B., and Yang, A. T., 1977. "Application of Instantaneous Invariants to the Analysis and Synthesis of Mechanisms". *ASME Journal of Engineering for Industry*, **99**, February, pp. 97–103.
- [6] Stanisic, M. M., Lodi, K., and Pennock, G. R., 1992. "Application of Curvature Theory to the Trajectory Generation Problem of Robot Manipulators". *ASME Journal of Mechanical Design*, **114**, December, pp. 677–680.
- [7] Lorenc, S. J., and Stanisic, M. M., 1994. "Third-Order Control of a Planar System Tracking Constant Curvature Paths". In *Advances in Robot Kinematics and Computational Geometry*, J. Lenarcic and B. Ravani, eds. Kluwer Academic Publishers, Dordrecht, pp. 229–238.
- [8] Lorenc, S. J., and Stanisic, M. M., 1994. "Second Order Geometry-Based Path Tracking of Industrial Arm Subassemblies". *23rd ASME Biennial Mechanisms Conferences*, **72**, September, pp. 301–306.
- [9] Chiaverini, S., Oriolo, G., and Walker, I. A. D., 2008. "Kinematically Redundant Manipulators". In *Springer Handbook of Robotics*, B. Siciliano and O. Khatib, eds. Springer Verlag, Western Europe, Chapter 11, pp. 245–268.
- [10] Nayak, J. H., and Roth, B., 1981. "Instantaneous Kinematics of Multiple-Degree-of-Freedom Motions". *ASME Journal of Mechanical Design*, **103**, July, pp. 608–620.
- [11] Stanisic, M. M., Pennock, G. R., and Krousgrill, C. M., 1988. "Inverse Velocity and Acceleration Solutions of Serial Robot Arm Subassemblies Using the Canonical Coordinate System". *International Journal of Robotics Research*, **7**(1), pp. 29–41.

- [12] Pennock, G. R., and Yang, C. M., 1988. “Instantaneous Kinematics of Three-Parameter Motions”. *Journal of Mechanisms, Transmissions, and Automation in Design*, **107**, June, pp. 157–162.
- [13] Atkeson, C. G., and Hollerbach, J. M., 1985. “Modeling Time Invariance in Human Arm-Motion Coordination”. *Journal of Neuroscience*, **5**(9), pp. 2381–2330.
- [14] Ambike, S. S., and Schmiedeler, J. P., 2006. “Modeling Time Invariance in Human Arm-Motion Coordination”. In *Advances in Robot Kinematics*, J. Lenarcic and B. Roth, eds. Springer, Dodrecht, pp. 177–184.
- [15] Pogorelov, A. V., 1966. *Differential Geometry*. P. Nordhoff N. V., Gronongen, The Netherlands.
- [16] Stoker, J. J., 1969. *Differential Geometry*. John Wiley & Sons, Inc., USA.
- [17] Ambike, S., and Schmiedeler, J. P., 2007. “First-Order Coordination of the Articulated-Arm Subassembly Using Curvature Theory”. Proceedings of the ASME 2007 International Design Engineering Technical Conferences & Computers and Information in Engineering Conference. Paper number DETC2007-34513.
- [18] Johnson, W. P. “The Curious History of Faa di Bruno’s Formula”. *The American Mathematical Monthly*, **109**, March, pp. 217–234.
- [19] Porteous, I. R., 2001. *Geometric Differentiation*. Cambridge University Press, Cambridge, UK.
- [20] Kecskeméthy, A., and Tandl, M., 2006. “A Robust Model for 3d Tracking in Object Oriented Multibody Systems Based on Singularity-Free Frenet Mapping”. In *Advances in Robot Kinematics*, J. Lenarcic and B. Roth, eds. Springer, Dodrecht, pp. 255–264.
- [21] Ambike, S., and Schmiedeler, J. P. “A Methodology for Implementing the Curvature Theory Approach to Path Tracking with Planar Robots”. *Mechanisms and Machine Theory*, **43**, October, pp. 1225–1235.
- [22] Mishkov, R. L., 2000. “Generalization of the Formula of Faa di Bruno for a Composite Function With a Vector Argument”. *Internat. J. Math. and Math. Sci.*, **24**(7), pp. 481–491.

## Appendix A

It is shown that the  $p^{th}$ -order coordination equation is always linear in the  $p^{th}$ -order speed ratios. The forward kinematic map can be viewed as a composite function with a vector argument:  $\bar{r}(\lambda) = \bar{r}(v(\lambda), \lambda(\lambda), \mu(\lambda), \cdot)$ , where  $\lambda(\lambda) = \lambda$  and  $\mu(\lambda)$  and  $v(\lambda)$  are the Taylor series given by Eqn. (2). When all the appropriate derivatives are defined, the generalized Faa-di-Bruno formula is used to obtain the  $p^{th}$ -derivative of a component  $r_m$

( $m = 1, 2, 3$ ) of  $\bar{r}(\lambda)$  as [22],

$$\frac{d^p r_m}{d\lambda^p} = \sum_0^p \sum_1^p \sum_2^p \cdots \sum_p^p \left( \frac{p!}{\prod_{i=1}^p (i!)^{g_i} \prod_{i=1}^p \prod_{i=1}^3 q_{ip}!} \cdot \frac{\partial^f r_m}{\partial \lambda^{p_1} \partial \mu^{p_2} \partial v^{p_3}} \right) \times \prod_{i=1}^p (\lambda^{(i)})^{q_{i1}} (\mu^{(i)})^{q_{i2}} (v^{(i)})^{q_{i3}}, \quad (24)$$

where the respective sums are over all non-negative integer solutions of the Diophantine equations as follows

$$\begin{aligned} \sum_0 &\rightarrow g_1 + 2g_2 + 3g_3 + \dots + pg_p = p, \\ \sum_1 &\rightarrow q_{11} + q_{12} + q_{13} = g_1, \\ \sum_2 &\rightarrow q_{21} + q_{22} + q_{23} = g_2, \\ &\vdots \\ \sum_p &\rightarrow q_{p1} + q_{p2} + q_{p3} = g_p, \end{aligned} \quad (25)$$

and  $p_1, p_2$ , and  $p_3$ , the orders of partial derivatives with respect to  $\lambda, \mu$ , and  $v$ , respectively, and  $f$ , the order of the partial derivative, are

$$\begin{aligned} p_e &= q_{1e} + q_{2e} + \dots + q_{pe}, \quad e = 1, 2, 3, \\ f &= p_1 + p_2 + p_3 = \sum_{i=1}^p g_i, \end{aligned}$$

and  $\mu^{(i)} := \frac{d^i \mu}{d\lambda^i}$ . Thus, only the last term in Eqn. (24) consists of the speed ratios. The condition  $i = p$  gives the highest-order speed ratio. Next, note that the sum  $\sum_0$  in Eqn. (25) implies that  $g_p$  can have no solution other than  $g_p = 0$  or 1. This, along with the sum  $\sum_p$  in Eqn. (25) implies that only one of the powers  $q_{p1}, q_{p2}$ , and  $q_{p3}$  can equal 1, and the other two must be zero. Therefore, for  $i = p$ , only one of the speed ratios in the last term of Eqn. (24) will remain and the others will equal 1. Therefore, the  $p^{th}$ -derivative of  $r_m$  will be linear in the  $p^{th}$ -order speed ratios.

Next, it is shown that the three component equations of a coordination equation of any order are consistent. Note that Eqn. (10) implies that  $\bar{X}$  is normal to  $\hat{T}$ . Next, since  $\bar{r}_{(\lambda\lambda\lambda\dots p \text{ times})0}$  is linear in the  $p^{th}$ -order speed ratios, let

$$\bar{r}_{(\lambda\lambda\lambda\dots p \text{ times})0} = \begin{bmatrix} u_1 n^{(p)} + v_1 k^{(p)} + w_1 \\ u_2 n^{(p)} + v_2 k^{(p)} + w_2 \\ u_3 n^{(p)} + v_3 k^{(p)} + w_3 \end{bmatrix},$$

where  $u_i, v_i$  and  $w_i$  are scalars. Then, the determinant corresponding to the system of equations in Eqn. (10) is given by,

$$det = (\bar{X} \cdot \hat{T})(\hat{T} \cdot \begin{bmatrix} u_2 v_3 - u_3 v_2 \\ u_3 v_1 - u_1 v_3 \\ u_1 v_2 - u_2 v_1 \end{bmatrix}).$$

Since  $\bar{X}$  is always normal to  $\hat{T}$ , the term  $\bar{X} \cdot \hat{T} = 0, \Rightarrow det = 0$ . Therefore, the component equations of the coordination equation of any order are always consistent. Note that this result holds for non-singular poses of the mechanism, i.e. when the Jacobian in Eqn. (11) is full rank.

$$\begin{aligned} A_\lambda(1) &= a_2 S_{\lambda_0} C_{v_0} + 3a_2 k C_{\lambda_0} S_{v_0} + 2k^{(2)} a_2 S_{\lambda_0} S_{v_0} \\ &\quad + 3k^2 a_2 S_{\lambda_0} C_{v_0} - 2kk^{(2)} C_{v_0} |\bar{Q}| + k^3 S_{v_0} |\bar{Q}| \\ &\quad + 3(1+n)k^2 a_3 S_{\psi_0} C_{v_0} + 3(1+n)^2 k a_3 C_{\psi_0} S_{v_0} \\ &\quad + 2(1+n)k^{(2)} a_3 S_{\psi_0} S_{v_0} - 2(1+n)n^{(2)} a_3 C_{\psi_0} C_{v_0} \\ &\quad + (1+n)^3 a_3 S_{\psi_0} C_{v_0} + 2n^{(2)} k a_3 S_{\psi_0} S_{v_0}, \\ A_\lambda(2) &= a_2 S_{\lambda_0} S_{v_0} - 3a_2 k C_{\lambda_0} C_{v_0} - 2k^{(2)} a_2 S_{\lambda_0} C_{v_0} \\ &\quad + 3k^2 a_2 S_{\lambda_0} S_{v_0} - 2kk^{(2)} S_{v_0} |\bar{Q}| - k^3 C_{v_0} |\bar{Q}| \\ &\quad + 3(1+n)k^2 a_3 S_{\psi_0} S_{v_0} - 3(1+n)^2 k a_3 C_{\psi_0} C_{v_0} \\ &\quad - 2(1+n)k^{(2)} a_3 S_{\psi_0} C_{v_0} - 2(1+n)n^{(2)} a_3 C_{\psi_0} S_{v_0} \\ &\quad + (1+n)^3 a_3 S_{\psi_0} S_{v_0} - 2n^{(2)} k a_3 S_{\psi_0} C_{v_0}, \\ A_\lambda(3) &= -a_2 C_{\lambda_0} - 2a_3(1+n)n^{(2)} S_{\psi_0} - a_3(1+n)^3 C_{\psi_0}, \\ D_\lambda(1) &= -a_3(1+n)C_{\psi_0} C_{v_0} + a_3 k S_{\psi_0} S_{v_0}, \\ D_\lambda(2) &= -a_3(1+n)C_{\psi_0} S_{v_0} - a_3 k S_{\psi_0} C_{v_0}, \\ D_\lambda(3) &= -a_3(1+n)S_{\psi_0}, \\ H_\lambda(1) &= [a_2 S_{\lambda_0} + a_3(1+n)S_{\psi_0}]S_{v_0} - k^{(2)} |\bar{Q}| C_{v_0}, \\ H_\lambda(2) &= [a_2 S_{\lambda_0} + a_3(1+n)S_{\psi_0}]C_{v_0} - k^{(2)} |\bar{Q}| S_{v_0}, \\ H_\lambda(3) &= 0. \end{aligned}$$

## Appendix B

The functions appearing in Eqn. (19) and Eqn. (20) are defined here.

$$\begin{aligned} A(1) &= -a_2 C_{\lambda_0} C_{v_0} + k(2a_2 S_{\lambda_0} S_{v_0}) \\ &\quad - k^2(a_2 C_{\lambda_0} C_{v_0} + a_3 C_{\psi_0} C_{v_0}) \\ &\quad + (1+n)(2a_3 k S_{\psi_0} S_{v_0}) - (1+n)^2(a_3 C_{\psi_0} C_{v_0}), \\ A(2) &= -a_2 C_{\lambda_0} S_{v_0} - k(2a_2 S_{\lambda_0} C_{v_0}) \\ &\quad - k^2(a_2 C_{\lambda_0} S_{v_0} + a_3 C_{\psi_0} S_{v_0}) \\ &\quad - (1+n)(2a_3 k S_{\psi_0} C_{v_0}) - (1+n)^2(a_3 C_{\psi_0} S_{v_0}), \\ A(3) &= -a_2 S_{\lambda_0} - a_3(1+n)^2 S_{\psi_0}, \\ D(1) &= -a_3 S_{\psi_0} C_{v_0}, \quad D(2) = -a_3 S_{\psi_0} S_{v_0}, \quad D(3) = a_3 C_{\psi_0}, \\ H(1) &= -|\bar{Q}| S_{v_0}, \quad H(2) = |\bar{Q}| C_{v_0}, \quad H(3) = 0. \end{aligned}$$